JOURNAL OF SOLID STATE CHEMISTRY **132,** 337–341 (1996)
ARTICLE NO. SC977471

Structure and Magnetic Properties of Tetravalent Praseodymium Perovskite $SrPrO_3$

Yukio Hinatsu[1] and Masahiro Itoh

Division of Chemistry, Graduate School of Science, Hokkaido University, Sapporo 060, Japan

and

Norman Edelstein

Chemical Sciences Division, Lawrence Berkeley Laboratory, University of California, Berkeley, California 94720

Received January 24, 1997; in revised form May 2, 1997; accepted May 12, 1997

The crystal structure of a tetravalent praseodymium perovskite $SrPrO_3$ has been investigated by powder X-ray diffraction using Rietvelt analysis method; it is orthorhombic ($a = 6.1168(8)$, $b = 8.5487(9)$, $c = 5.9857(7)$ Å) with the space group *Pbnm*. The distortion from the ideal cubic perovskite structure for $SrPrO_3$ is much larger than that for $BaPrO_3$; the octahedral array of oxygen ions about Pr^{4+} is considerably distorted in $SrPrO_3$. The magnetic susceptibility measurements of $SrPrO_3$ show no existence of the magnetic ordering down to 2.0 K. This is in contrast to the result of isomorphous $BaPrO_3$ which shows an antiferromagnetic transition at 11.5 K. The electron paramagnetic resonance (EPR) spectrum of the Pr^{4+} could be measured by doping it in an isomorphous $SrCeO_3$ which is diamagnetic and lowering the temperature to 4.2 K. The EPR spectrum was anisotropic, which corresponds to the deviation of the octahedral oxygen coordination symmetry around the Pr^{4+} ion. The *g* values obtained are discussed in terms of the crystal field theory.

INTRODUCTION

The most stable oxidation state of lanthanide elements is trivalent. In addition to this state, cerium, praseodymium, and terbium have the tetravalent state (1). We are interested in the electronic state of tetravalent praseodymium ions in solids.

The electronic configuration of the tetravalent praseodymium ion is $[Xe]4f^1$ ([Xe]: xenon electronic core). For electronic structure analysis, this f^1 configuration is straightforward as only the crystal field and spin–orbit coupling interaction are important. Especially, in the case when this ion is located in an octahedral crystal field environment, such a compound is suitable for studying the behavior of the 4*f* electron in solids because it is easy to compare the experimental results with theoretical calculation.

Perovskite-type oxides, ABO_3, where *A* is a divalent ion (e.g., Sr, Ba), accommodate tetravalent metal ions at the *B* site of the crystal (2).

In an earlier study (3), we reported that the barium praseodymium oxide $BaPrO_3$ shows an antiferromagnetic transition at 11.5 K. Since the 4*f* electron is effectively screened by the outer $5s^25p^6$ shells, the magnetic ordering temperature is usually very low when a magnetic cooperative phenomenon exists: 11.5 K is considerably high as the magnetic transition temperature of a lanthanide compound. Above the transition temperature, the susceptibility follows the modified Curie–Weiss law and the effective magnetic moment of Pr^{4+} in $BaPrO_3$ is $0.68\ \mu_B$. This result means that although the paramagnetic property of this compound is attributable to an unpaired 4*f* electron, the effect of the crystal field on the Pr^{4+} ion is great. To clarify the nature of the 4*f* electron to which the magnetic properties of lanthanide compounds are attributable, we tried to measure an electron paramagnetic resonance (EPR) spectrum of the tetravalent praseodymium ion (4). The EPR spectrum of Pr^{4+} ion in an octahedral crystal field could be successfully measured by doping it in the perovskite $BaCeO_3$ (where the Pr^{4+} ion is substituted for the Ce^{4+} ion) and by lowering the experimental temperature down to liquid helium temperature. In the EPR spectrum, a very large hyperfine interaction with the ^{141}Pr nucleus (nuclear spin $I = 5/2$) was measured.

In this study, we have paid attention to the strontium praseodymium oxide $SrPrO_3$. Although the symmetry of

[1]To whom correspondence should be addressed.

0022-4596/97 $25.00

the $SrPrO_3$ is orthorhombic, its crystal structure has not yet been determined. In this experiment, we cautiously prepared the oxygen stoichiometric $SrPrO_3$ and measured the powder X-ray diffraction. The X-ray diffraction results were analyzed using Rietvelt method. The magnetic susceptibility and electron paramagnetic resonance spectrum for $SrPrO_3$ were measured to elucidate the magnetic behavior of the 4*f* electron in solids. By comparing the magnetic properties of $SrPrO_3$ with those of $BaPrO_3$, we will discuss the effect of the crystal distortion from ideal cubic perovskite structure on the behavior of the 4*f* electron in solids.

EXPERIMENTAL

1. Sample Preparation

$SrPrO_3$. $SrCO_3$ and Pr_6O_{11} were used as the starting materials. Before use, the Pr_6O_{11} was heated in air at 1000°C for 8 h to remove any moisture. They were weighed in the correct metal ratio, intimately mixed, and heated in a flowing oxygen atmosphere at 1300°C in an SiC resistance furnace for a day. After cooling to room temperature, the sample was crushed into powder, reground, repressed into pellets, and heated under the same conditions to make the reaction complete. Since the $SrPrO_3$ loses a few oxygen atoms at high temperatures and is oxidized to the stoichiometric composition during cooling, the sample was first kept at 1000°C for 48 h, at 750°C for 48 h, and then cooled to room temperature in the furnace (5).

$SrPr_{0.02}Ce_{0.98}O_3$. For the EPR measurements, the $SrPrO_3$ was diluted with a diamagnetic $SrCeO_3$. $SrCO_3$, Pr_6O_{11}, and CeO_2 were used as the starting materials. The CeO_2 was heated in air at 850°C to remove any moisture and oxidized to the stoichiometric composition. They were weighed in the correct metal ratio, intimately mixed, and heated in a flowing oxygen atmosphere at 1300°C for 1 day. The sample was kept at 1000°C for 24 h and then cooled to room temperature in the furnace.

2. X-Ray Diffraction Analysis

Powder X-ray diffraction patterns were recorded on a Rigaku RINT2000 diffractometer using Cu$K\alpha$ radiation which was monochromatized by a curved graphite crystal.

3. Magnetic Susceptibility Measurements

The temperature dependence of the magnetic susceptibilities was measured both with a Faraday-type torsion balance and with a commercial SQUID magnetometer (Quantum Design, MPMS model).

The temperature range of the magnetic susceptibility measurements with the magnetic balance was between 4.2 K and room temperature. The apparatus was calibrated with $CoHg(SCN)_4$ as a standard (6). The temperature of the sample was measured by a "normal" Ag vs Au 0.07 at.% Fe thermocouple (4.2 ~ 40 K) (7) and an Au–Co vs Cu thermocouple (10 K ~ room temperature).

The magnetic susceptibility measurements with the SQUID magnetometer were carried out at 1000 G in the temperature range between 2.0 and 300 K.

Magnetic susceptibility measurements with both the magnetic torsion balance and the SQUID magnetometer gave the same results.

4. Electron Paramagnetic Resonance Measurements

The EPR measurements were carried out with a JEOL RE-2X spectrometer operating at X-band frequency (~9.1 GHz) with 100-kHz field modulation. Measurements were made both at room temperature and at 4.2 K. The magnetic field was swept from 100 to 13,500 G. Before the specimen was measured, a blank was recorded to eliminate the possibility of interference by the background resonance of the cavity and/or sample tube. The magnetic field was monitored with a proton NMR gaussmeter, and the microwave frequency was measured with a frequency counter.

RESULTS AND DISCUSSION

The crystal structure of a tetravalent praseodymium perovskite $SrPrO_3$ has been investigated by powder X-ray diffraction using Rietvelt method. Indexing of the powder X-ray diffraction pattern obtained was accomplished with the aid of a computer program CELL (8). Structural refinements were performed with a Rietvelt program RIETAN (9). $SrPrO_3$ is orthorhombic ($a = 6.1168(8)$, $b = 8.5487(9)$, $c = 5.9857(7)$ Å) with the space group *Pbnm*. The atomic positions, and some important bond lengths and angles are listed in Table 1. It was found that the results on the crystal structure of $SrPrO_3$ were not very much different from those on $BaPrO_3$. Figure 1 shows the crystal structure of $SrPrO_3$ determined in this study. The ideal perovskite ABO_3 can be viewed as a three-dimensional network of *B*–O corner-sharing, with the *B* ion sitting in a site of Oh symmetry. The orthorhombic distortion observed in the present compound involves a cooperative buckling of these corner-sharing octahedra, as shown in Fig. 1. For the case of $BaPrO_3$, however, there are only small changes in the near-neighbor oxygen coordination about the Pr site; the Pr^{4+} ions have an almost octahedral arrangement of near-neighbor oxygen ions. In contrast, in the $SrPrO_3$, the distortion from ideal cubic perovskite is much larger than that for $BaPrO_3$; the oxygen coordination symmetry around the Pr^{4+} is no longer octahedral. Detailed crystal structure data for not only the $SrPrO_3$ but also the solid solutions $Sr_{1-x}Ba_xPrO_3$ will be described elsewhere (5).

TABLE 1
Atomic Positions, Bond Lengths, and Bond Angles for $SrPrO_3$

Atomic positions				
Atoms	Sites	x	y	z
Sr	4c	− 0.006	0.044	0.250
Pr	4b	0.000	0.500	0.000
O(1)	4c	0.121	0.479	0.250
O(2)	8d	0.685	0.322	0.048
Bond lengths (Å)				
Sr–O(1)	2.340 (×1)	2.762 (×1)	3.543 (×1)	3.703 (×1)
Sr–O(2)	2.444 (×2)	2.909 (×2)	3.048 (×2)	3.901 (×2)
Pr–O(1)	2.260 (×2)			
Pr–O(2)	2.216 (×2)	2.297 (×2)		
Bond angles (°)				
Pr–O(1)–Pr	142.02			
Pr–O(2)–Pr	142.92			

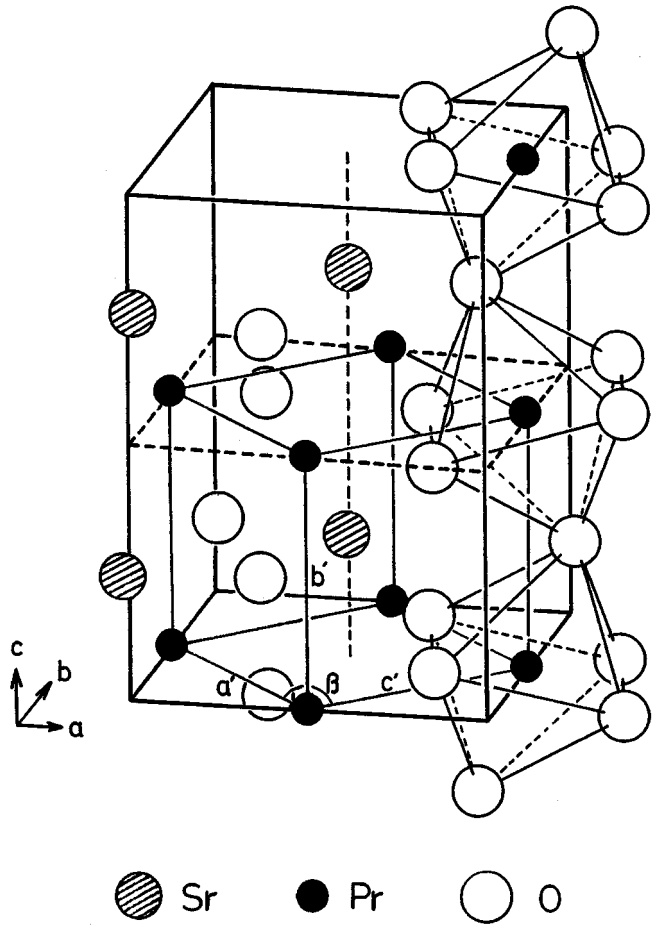

FIG. 1. Crystal structure of $SrPrO_3$.

Figure 2 shows the temperature dependence of the magnetic susceptibility for $SrPrO_3$ together with that for $BaPrO_3$ in the lower temperature range. $SrPrO_3$ shows no magnetic ordering in the experimental temperature range and its susceptibility increases with decreasing temperature down to 2.0 K. This result contrasts with that for $BaPrO_3$, which shows long-range magnetic ordering at 11.5 K (3). In the latter case, the alignment of Pr^{4+}–O^{2-}–Pr^{4+} is approximately linear, so the antiferromagnetic ordering (180° superexchange interaction) occurs at high temperature. In the $SrPrO_3$, the alignment of Pr^{4+}–O^{2-}–Pr^{4+} is no longer linear (see Fig. 1), so the magnetic ordering temperature is expected to be very low even if the magnetic exchange interaction between praseodymium ions operates through oxygen ions. From the temperature-dependent part of the magnetic susceptibility, the effective magnetic moment of praseodymium is obtained to be 1.57 μ_B, which is often found for compounds of which the unpaired electron is an f^1 electron.

An EPR experiment was carried out in order to know the behavior of the 4f electron in the solid in more detail. For the praseodymium ion in the tetravalent state, an EPR spectrum should be observed because the Pr^{4+} ion is a Kramers ion ([Xe]$4f^1$ configuration). However, no EPR spectra were observed even at 4.2 K for pure $SrPrO_3$, which is probably due to the dipole–dipole interaction of tetravalent praseodymium ions (10). Therefore, we have prepared a sample in which Pr^{4+} ions were doped in $SrCeO_3$ (which is isomorphous with $SrPrO_3$) and we have lowered the experimental temperature to measure the EPR spectra down to liquid helium temperature. The EPR spectra could be measured at 4.2 K. With increasing temperature, all the assigned absorption EPR lines become weaker in intensity considerably. This observation of an EPR spectrum strongly indicates that the oxidation state of the praseodymium ion is not trivalent, but tetravalent, because the non-Kramers Pr^{3+} ion usually shows no EPR spectrum (11).

Figure 3 shows the anisotropic EPR spectra for Pr^{4+}/$SrCeO_3$ (upper spectrum) measured at 4.2 K. For the case of Pr^{4+}/$BaCeO_3$, its EPR spectrum is isotropic (4). This difference directly reflects their crystal structures.

The crystal structure of $SrCeO_3$ is the same as that of $SrPrO_3$, i.e., it is orthorhombic as shown in Fig. 1. In the true crystallographic cell, there are four distorted perovskite pseudo-cells. They are monoclinic and their cell parameters are $a' = c' = 4.3010(10)$, $b' = 4.2936(10)$ Å, and $\beta = 91.36(3)°$ for Pr^{4+}/$SrCeO_3$, and $a' = c' = 4.3944(10)$, $b' = 4.3966(10)$ Å, and $\beta = 90.19(3)°$ for Pr^{4+}/$BaCeO_3$, which indicates that the distortion from ideal cubic perovskite structure is much larger for Pr^{4+}/$SrCeO_3$ and that we can no longer assume that the oxygen coordination symmetry around the Pr^{4+} ion is octahedral.

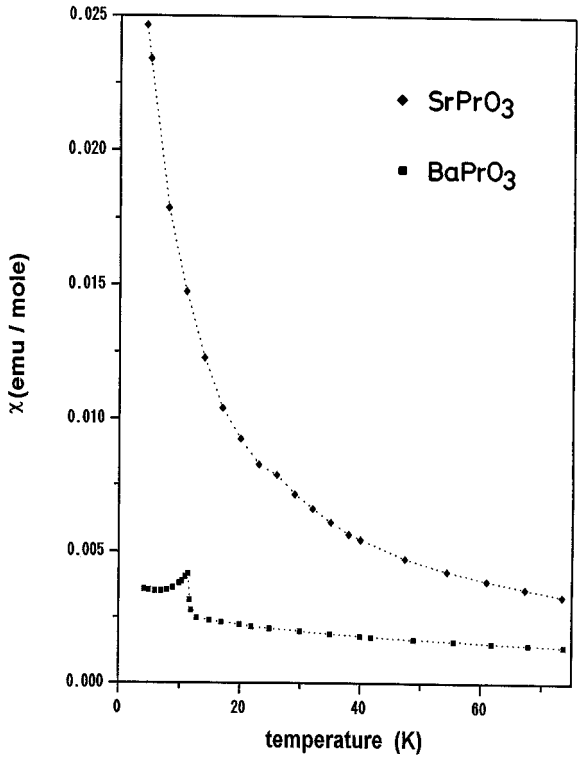

FIG. 2. Temperature dependence of magnetic susceptibilities for $SrPrO_3$ and $BaPrO_3$.

The spin Hamiltonian appropriate for the distorted octahedral site of Pr^{4+} in $SrCeO_3$ is (11)

$$H = S' \cdot g \cdot S' + S' \cdot A \cdot I + I \cdot Q \cdot I, \qquad [1]$$

where g, A, and Q are the g (or Zeeman), hyperfine, and quadrupole tensors, respectively. S' and I are the effective spin and nuclear spin quantum numbers, respectively. For the Pr^{4+} configuration, $S' = 1/2$ and the nuclear spin of ^{141}Pr is $I = 5/2$. The case for the spectrum of $Pr^{4+}/BaCeO_3$ in which the Pr^{4+} ion is at a site of octahedral symmetry showed that the hyperfine term cannot be regarded as a perturbation of the Zeeman term and the effective Hamiltonian has to be solved exactly (4). In the present low-symmetry case, the parameters that must be fitted are g_{xx}, g_{yy}, g_{zz}, A_{xx}, A_{yy}, A_{zz}, Q_{xx}, Q_{yy}, and Q_{zz}. The quadruple tensor contribution is expected to be small compared to the Zeeman and hyperfine terms and in the preliminary analysis is set equal to zero. The values of g_{xx}, g_{yy}, and g_{zz} were empirically varied to obtain a reasonable simulation to the experimental spectrum. The values of A_{xx}, A_{yy}, and A_{zz} were obtained by using the ratio of A/g for $Pr^{4+}/BaCeO_3$ (4), and assuming this ratio was the same for Pr^{4+} in $SrCeO_3$ (12). Thus, the values of the components of the A tensor are determined by the values of the g tensor: $|g_x| = 0.875$, $|g_y| = 0.790$, $|g_z| = 0.755$; $A_x = 0.0712$, $A_y = 0.0643$, $A_z = 0.0614\ cm^{-1}$. The results of the fitting are shown in Fig. 3. The lower spectrum is the one calculated. The fit is reasonable but not perfect. This is due to not solving the Hamiltonian exactly and the neglect of the quadrupole tensor. It appears that the experimental line at 6286 G cannot be accounted for even qualitatively. This fact suggests that this feature does not come from the Pr^{4+} ion.

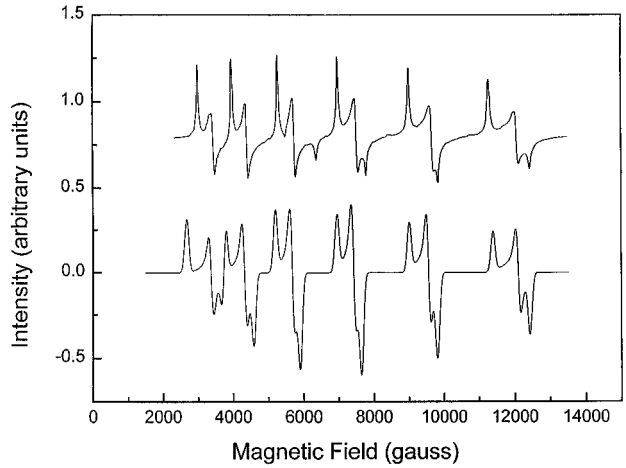

FIG. 3. EPR spectra for Pr^{4+} doped in $SrCeO_3$. Upper, experimental; lower, calculated.

Here, we will briefly discuss the g values obtained here. Although the anisotropic g values (i.e., $g_x \neq g_y \neq g_z$) means the distortion from octahedral symmetry at the Pr^{4+} site, we will consider the case of a single $4f$ electron in an octahedral crystal field. Figure 4 shows the effects of perturbing the f^1 orbital energy levels successively by an octahedral crystal field and spin–orbit coupling. The sevenfold orbitally degenerate energy state of the $4f$ electron is split into a singlet state Γ_2 and two triplet states Γ_4 and Γ_5, due to the octahedral crystal field. The energy difference between Γ_2 and Γ_5 is labeled Δ, and the energy difference between Γ_4 and Γ_5 is labeled Θ. When the spin–orbit coupling is taken into account, the Γ_2 orbital state is transformed into a doublet Γ_7, and the Γ_5 and Γ_4 states are split into Γ'_7 and Γ_8, and Γ_6 and Γ'_8, respectively (13). The ground state Kramers doublet is a Γ_7 state and is coupled to the excited Γ'_7 state, arising from the Γ_5 orbital state, by the spin–orbit coupling (with ζ the spin–orbit coupling constant). The g value for the ground state is calculated to be

$$g = 2\langle \Gamma_7 | L + 2S | \Gamma_7 \rangle = 2\cos^2\theta - 4/\sqrt{3}\sin 2\theta, \qquad [2]$$

where θ is the parameter describing the admixture of the Γ_7 levels in the ground state, determined by the relation

$$\tan 2\theta = 2\sqrt{3}/(\Delta - 1/2\zeta). \qquad [3]$$

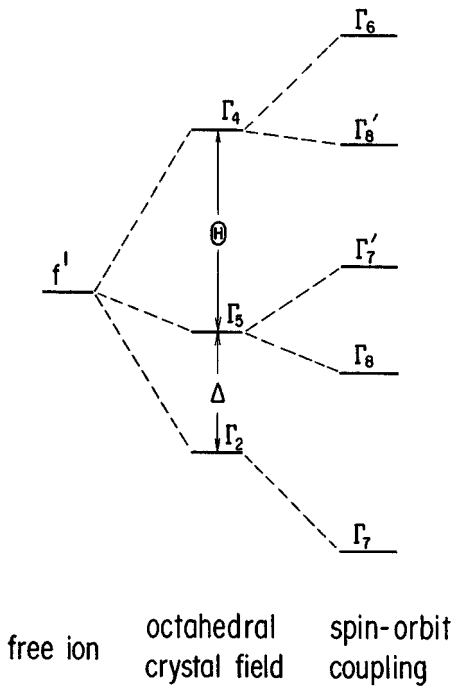

FIG. 4. Splitting of f^1 orbital perturbed by octahedral crystal field and spin–orbit coupling.

This equation indicates that the g value for an f electron perturbed by the octahedral crystal field should be between $-10/7$ (for the Γ_7 ground doublet in the $^2F_{5/2}$ multiplet) and 2.00 (no spin–orbit interaction), and it increases from $-10/7$ to 2.00 with increasing crystal field effect (14, 15). The $|g|$ values ($0.755 \sim 0.875$) means that they are reasonable for a $4f$ electron in the octahedral crystal field.

On the other hand, although the sign of the g value is not obtained by this experiment, comparison with other f^1 systems in octahedral symmetry, such as NpF_6/UF_6 (16) and Pa^{4+}/Cs_2ZrCl_6 (17), where the sign of the g value has been measured, indicates that the g value for the $Pr^{4+}/SrCeO_3$ should be negative. Therefore, the value of $|g|$ which is directly obtained from the EPR experiment, decreases with increasing crystal field strength. The fact that the $|g|$ values obtained here are much smaller than $|-10/7|$ indicates that the crystal field effect on the behavior of a $4f$ electron is large.

The major conclusion determined from the EPR spectrum of Pr^{4+} in $SrCeO_3$ is the distortion from octahedral symmetry at the Pr^{4+} site is of a much larger magnitude than in the $BaCeO_3$. In the latter case the EPR spectrum could be satisfactorily fit with a Hamiltonian representing O_h symmetry. In the present case a g value anisotropy of greater than 5% is needed to qualitatively simulate the observed spectrum.

This work is supported by the Asahi Glass Foundation.

REFERENCES

1. N. E. Topp, "Chemistry of the Rare-Earth Elements." Elsevier, Amsterdam, 1965.
2. J. B. Goodenough and J. M. Longo, *in* "Landolt–Börnstein Tabellen" (K.-H. Hellwege and A. M. Hellwege, Eds.), Neue Serie, III Band, 4a, Chap. 3. Springer-Verlag, Berlin, 1970.
3. Y. Hinatsu, *J. Solid State Chem.* **102**, 362 (1993).
4. Y. Hinatsu and N. Edelstein, *J. Solid State Chem.* **112,** 53 (1994).
5. M. Itoh and Y. Hinatsu, *J. Alloys Compounds.* [in press]
6. H. St. Rade, *J. Phys. Chem.* **77,** 424 (1973).
7. L. L. Sparks and R. L. Powell, *J. Res. Nat. Bur. Stand. A* **76,** 263 (1972).
8. Y. Takaki, T. Taniguchi, H. Yamaguchi, and T. Ogura, *Yogyo-Kyokaishi* **95,** 610 (1987).
9. F. Izumi, *Nippon Kesshou Gakkaishi* **27,** 23 (1985).
10. Another reason for the absence of the EPR spectrum for $SrPrO_3$ could be the existence of a certain Pr^{3+} ions combined with an equivalent quantity of oxygen vacancies.
11. A. Abragam and B. Bleaney, "Electron Paramagnetic Resonance of Transition Ions," Chap. 5. Oxford Univ. Press, London, 1970.
12. A. Abragam and B. Bleaney, "Electron Paramagnetic Resonance of Transition Ions," p. 297. Oxford Univ. Press, London, 1970.
13. B. R. Judd, "Operator Techniques in Atomic Spectroscopy," McGraw–Hill, New York, 1963.
14. Y. Hinatsu, T. Fujino, and N. Edelstein, *J. Solid State Chem.* **99,** 182 (1992).
15. Y. Hinatsu, *J. Alloys Compounds* **203,** 251 (1994).
16. C. A. Hutchison and B. Weinstock, *J. Phys. Chem.* **32,** 56 (1960).
17. J. D. Axe, H. J. Stapleton, and C. D. Jeffries, *Phys. Rev.* **121,** 1630 (1961).